Photoabsorption of atoms inside C_{60}

M. J. Puska and R. M. Nieminen

Laboratory of Physics, Helsinki University of Technology, 02150 Espoo, Finland

(Received 16 July 1992)

The photoabsorption spectrum of the C_{60} molecule and those of Xe and Ba atoms inside the C_{60} molecule are calculated using a jelliumlike model for the confining cage. The dynamic electronic response to an external electric field is obtained through time-dependent density-functional theory. The photoabsorption cross section for C_{60} shows strong collective resonances corresponding to plasmonlike excitations. The resonant $4d$ photoemission of the free atom is suppressed by the carbon cage, resulting in a weakly oscillating spectrum.

PACS number(s): 36.40.+d, 33.80.−b, 71.45.Gm

I. INTRODUCTION

The electronic structure of the C_{60} molecule and its condensed phases are well understood by first-principles calculations [1–3]. For example, the theoretical predictions and measurements are in good agreement for both the ground-state structures [4,5] and the excitation energies [3] of solid C_{60}. Recently, the photoabsorption spectrum of C_{60} molecules has been calculated [6] and measured [7]. The characteristic feature of both theory and experiment is a giant collective resonance around an unusually high energy of 20 eV.

One of the exciting properties of the C_{60} molecules is that it can confine metal atoms such as La, Ca, Ba, and Sr [8,9]. This will lead to differences between the measured properties of a free atom and the same atom inside the carbon cage. It is also important to understand the physical reasons for these differences. Theoretical calculations such as the present one can help to achieve this goal.

In this paper we report on calculations of the dynamic response function of the C_{60} molecule and atoms (Xe and Ba) placed inside the C_{60} sphere. We use the time-dependent density-functional theory (TD-DFT) [10,11], which is the state-of-the-art technique for calculating excitation spectra. We apply TD-DFT to obtain the photoabsorption cross section, employing a simple "jellium-shell" model for the C_{60} cage. The nucleus of the central atom is introduced as a point charge. It is argued that this model captures the essential physical features of the excitation spectrum and is even quantitatively accurate.

We have chosen to present Xe and Ba as central atoms for several reasons. First, in our model these atoms result in closed electron shell structures required in applying TD-DFT. Secondly, Xe and Ba show strong characteristic resonance photoabsorption from the $4d$ core levels [11–13]. Thirdly, Ba is adjacent to La, which is the first and most studied atom inside the C_{60} molecule [8,9]. The qualitative features in the resonance photoabsorption are not expected to change from Ba to La.

TD-DFT has been previously used in similar contexts for free atoms [10,11], for jellium spheres mimicking small metallic clusters [14,15], and for a uranium atom surrounded by a jellium sphere describing the metallic state [16]. The main phenomena of interest have been the excitation of collective plasmon modes (giant resonances) in metal clusters at low photon energies [14,15] and the photoabsorption cross section near core-level excitation thresholds, especially in the case of resonance absorption [11,16]. In this work we consider both of these aspects.

The outline of the present paper is as follows: In Sec. II we describe the spherical jellium-shell model used to describe the C_{60} molecule and compare the ground-state electronic properties with the first-principles results for the molecule. In Sec. III the main features of the TD-DFT are summarized. We have described the details of our approach before [15]. The results are presented and discussed in Sec. IV, and Sec. V is a short summary.

II. SPHERICAL MODEL FOR C_{60}

The first-principles calculations for the electronic structure of the C_{60} molecule are in excellent agreement with the photoemission [3,17] and inverse-photoemission [18] measurements. Martins, Troullier, and Weaver [19] have analyzed the electron wave functions from these calculations by making the decomposition of the different eigenstates into the function basis of spherical symmetry. They found that with a few exceptions the eigenfunctions of the valence band and the bottom of the conduction band are characterized mainly by a single angular momentum quantum number l. They were also able to extract the nodal structure of the eigenstates in the radial direction and thereby label the eigenfunctions with the principal quantum number n. The states without nodes in the radial direction, $n = 1$, correspond to the carbon σ orbitals, whereas the states with a node plane in the radial direction, $n = 2$, correspond to the π orbitals. On the basis of this analysis, Martins, Troullier, and Weaver [19] suggested that the C_{60} molecule could be modeled by a spherical shell with an attractive (screened) potential for electrons. The radius of the shell should be the radius of the C_{60} molecule ($R = 6.7a_0$) and the thickness of the shell about twice the atomic radius ($\Delta R = 2 \times 2.8a_0 = 5.6a_0$) of carbon.

We have further developed the spherical shell model

M. J. PUSKA AND R. M. NIEMINEN

for the C_{60} molecule. We introduce a shell of positive rigid background charge, jellium, which is symmetrically placed with respect to the radius R of the C_{60} molecule, i.e., the positive charge distribution $n_+(r)$ is

$$n_+(r) = \begin{cases} n_0, & \text{when } R - \dfrac{\Delta R}{2} \leq r \leq R + \dfrac{\Delta R}{2} \\ 0, & \text{otherwise .} \end{cases} \tag{1}$$

The thickness ΔR of the shell is determined by requiring charge neutrality with a given number of valence electrons. The background density or the corresponding density parameter $r_s = (\frac{4}{3}\pi n_0)^{-1/3}$ is then left as an adjustable parameter.

The results obtained by jellium models, while qualitatively very useful, can sometimes lead to unphysical conclusions [20]. For quantitatively accurate results, corrections beyond the jellium model have to be introduced. One possibility is to introduce the ionic pseudopotentials within perturbation theory [20]. The main influence of the pseudopotentials can also be taken into account in calculating the self-consistent electron density either in a variational procedure [21] or spherically averaging the pseudopotentials in order to retain high symmetry [22]. In this work we describe the effects of the ion cores by introducing an extra external potential v_{ps} inside the jellium shell:

$$v_{ps}(r) = \begin{cases} -v_0, & \text{when } R - \dfrac{\Delta R}{2} \leq r \leq R + \dfrac{\Delta R}{2} \\ 0, & \text{otherwise .} \end{cases} \tag{2}$$

The depth of the potential well, v_0, is the other adjustable parameter in our model.

The total effective potential in the calculations is

$$v_{\text{eff}}(r) = \int \frac{n_-(r') - n_+(r')}{|\mathbf{r} - \mathbf{r}'|} 4\pi r^2 dr' + v_{ps}(r) - Z/r \ , \tag{3}$$

where the possibility of placing an atom with nuclear charge Z in the center of the C_{60} molecule is taken into account. The ground-state electron density $n_-(r)$ of the system is solved self-consistently within the local-density approximation [23] (LDA) of the density-functional theory [24]. In the case of an atom inside the carbon cage, the self-consistency cycle includes all the free atom-like states (also the deep core states) and states which are mostly localized near the jellium shell. The self-consistent solution leads to hybridization of these two types of states. In this sense the present model resembles that in Ref. [16].

The parameters r_s and v_0 should be chosen so that the properties of the model system resemble as much as possible those of the C_{60} molecule derived from the first-principles calculations (and from measurements). We have chosen for our presentation a system of 250 electrons which has closed electron shells and which is obtained using the parameter values $r_s = 1.2a_0$ and $v_0 = 0.7$ hartree. The spectrum of bound energy levels of this spherical-jellium shell-system is shown in Fig. 1, which also gives the degeneracies $[2(2l+1)]$. States with $n = 1$
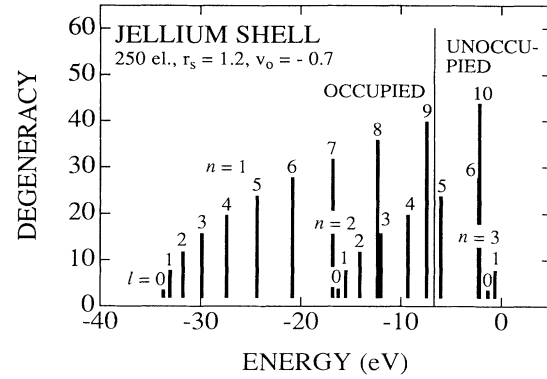

FIG. 1. One-electron energy spectrum of a jellium shell with 250 electrons. The model parameters (see text) are $r_s = 1.2a_0$ and $v_0 = 0.7$ hartree. The zero of energy corresponds to the bottom of the conduction band. The heights of the bars give the degeneracies $2(2l+1)$ of the states.

(σ states) are occupied up to $l = 9$ and states with $n = 2$ (π states) up to $l = 4$. In the C_{60} molecule there are 240 valence electrons. According to Martins, Troullier, and Weaver [19], the nonspherical components of the real system split noticeably the σ levels and π levels with $l \geq 5$ and $l \geq 3$, respectively. The resulting $l = 9$ σ- and $l = 5$ π-derived levels are only partly occupied, which results in a system of 240 valence electrons. One should also note that in some cases, especially for the continuum states, the character of the resulting state cannot be specified to correspond to a single state of spherical symmetry, but is a mixing of several states [19].

The level schemes for σ and π states shown in Fig. 1 are close to that arising for two-dimensional electron gas on a spherical surface. In this case the energy eigenvalues depend on the quantum number l as $E_l = l(l+1)/2R^2$ (in atomic units). The spacings between the highest actual energy levels in Fig. 1 are, due to the finite depth and smoothening of the potential well (Fig. 2), slightly smaller than those given by this simple equation.

The energy spectrum of the model system resembles that of the first-principles calculations and the experimental findings in many ways.

(i) The energy spread of the occupied valence-electron levels of the C_{60} molecule is, according to LDA calculations [1], about 20 eV. This energy spread is conserved also in the solid state formed by C_{60} molecules [2,3]. The energy spread of the occupied orbitals in the spherical model is slightly larger, presumably due to the lack of the energy-level splitting.

(ii) The width of the occupied spectrum of the π states also agrees well with the first-principles estimates. As a matter of fact, the valence-electron orbitals cannot be separated to the σ and π orbitals on the basis of symmetry as in the case of graphite. Saito and Oshiyama [2] concluded on the basis of the enhanced dispersion of the solid-state energy bands that the π orbitals span the energy region from 6 eV below the highest occupied level to 7 eV about that level. The analysis of Martins, Troullier, and Weaver [19] gave a similar result with a slightly
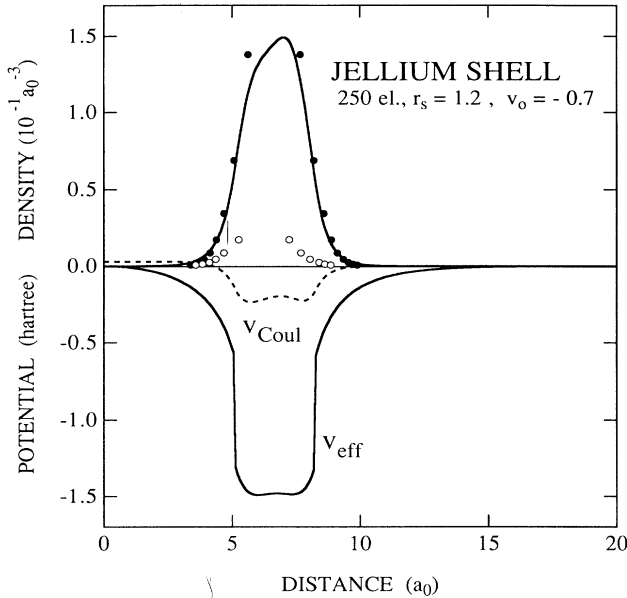
FIG. 2. Self-consistent electron density and effective potential with its Coulombic part for a jellium shell with 250 electrons. The electron density is compared with the valence-electron density from a pseudopotential calculation [2] along a radial line bisecting the bond between two carbon atoms (solid circles) or going through the center of a carbon-atom hexagon (open circles).

larger energy spread.

(iii) The position of the highest occupied levels with respect to the vacuum (the energy zero in Fig. 1) is in agreement with the measured ionization potential of 7.5–7.7 eV of the C_{60} molecule [25,7] and the absolute position 7.3–7.6 eV of the Fermi level in the solid C_{60} [3,26].

(iv) The estimates for the lowest excitation energies calculated from our one-electron energy spectrum are 3.29 and 5.24 eV for $n=2$, $l=4\rightarrow n=2$, $l=5$ and $n=1$, $l=9\rightarrow n=1$, $l=10$ transitions, respectively. It is tempting to complement this list with the transitions $n=2$, $l=5\rightarrow n=2$, $l=6$ and $n=1$, $l=8\rightarrow n=1$, $l=9$ with energies 3.79 and 4.91 eV, respectively. These transitions are not possible in our model, but their counterparts are allowed in the real system because of the partial occupancy of $n=1$, $l=9$ and $l=5$, $n=2$ derived states. These four excitation energies can be compared with the experimental peaks at 3.06, 3.76, 4.82, and 5.85 eV [27].

(v) Our spherical model also shows $n=3$ states just below the vacuum level. This is in agreement with the finding of Martins, Troullier, and Weaver [19] that 2.7 eV above the conduction-band minimum in the solid C_{60}, there exists a state which has neither σ nor π character. The wave function of this state is localized inside the C_{60} molecule. In our spherical model the $n=3$ states have this character, too.

The self-consistent potential and electron density for the jellium shell of 250 electrons are shown in Fig. 2. Within the shell, the largest contribution to the total effective potential is due to the pseudopotential part. The

potential well is noticeably rounded at its upper parts due to Coulomb and exchange-correlation contributions. The electron density is peaked around the potential well. The spherical electron density represents an average over different directions in the actual C_{60} molecule. This aspect is stressed in Fig. 2 by comparing the jellium-shell electron density with the density of the actual C_{60} molecule [2] in two different directions. It is especially gratifying that the spherical density decays outside the jellium shell as well as towards to the center of the shell similarly as the density of the molecule. This is important because we want to study the interaction of an atom inserted in the center of the molecule with the C-atom cage.

III. RESPONSE FUNCTION AND PHOTOABSORPTION

We have calculated the response function of the pure jellium shell and the shells containing impurity atoms in an external field using TD-DFT [10,11]. In particular, we obtain the dipolar polarizability and the photoabsorption cross section. The noninteracting electron response function $\chi^0(\mathbf{r},\mathbf{r}',\omega)$ of the system is first calculated for the frequency ω of the external field. This involves summations over occupied states only, when Green's functions calculated from both outgoing and incoming spherical waves are used [10,11]. Then the Hartree field and the exchange-correlation interaction (within LDA) are included, and the interacting electron response function $\chi(\mathbf{r},\mathbf{r}',\omega)$ is solved from the Dyson equation (in practice, by a matrix inversion). When the response function is known, the electron density $\delta n(\mathbf{r},\omega)$ induced by the dynamic external field $\delta v_{ext}(\mathbf{r},\omega)$ is obtained as

$$\delta n(\mathbf{r},\omega)=\int \chi(\mathbf{r},\mathbf{r}',\omega)\delta v_{ext}(\mathbf{r}',\omega)d\mathbf{r}' . \tag{4}$$

The relevant perturbation has the form

$$\delta v_{ext}(\mathbf{r},\omega)=\mathbf{E}_0\cdot\mathbf{r}e^{-i\omega t} ,$$

where $\mathbf{E}_0$ is the electric-field amplitude. In this case the dipolar component of the response function is sufficient. The induced dipole moment is then

$$\mathbf{p}(\omega)=-\int \mathbf{r}\delta n(\mathbf{r},\omega)d\mathbf{r}=\alpha(\omega)\mathbf{E}_0 , \tag{5}$$

where $\alpha(\omega)$ is the frequency-dependent polarizability. In general, $\alpha(\omega)$ is a complex quantity and its imaginary part gives the photoabsorption cross section as

$$\sigma(\omega)=4\pi\frac{\omega}{c}\text{Im}[\alpha(\omega)] , \tag{6}$$

where c is the speed of light.

IV. RESULTS AND DISCUSSION

A. C_{60} molecule

According to our calculations, the static polarizability $\alpha(\omega=0)$ of the jellium shell of 250 electrons (and with parameters $r_s=1.2a_0$ and $v_0=0.7$ hartree) is $618a_0^3$. This is somewhat larger than the lower limit estimation of $422a_0^3$ from quantum-mechanical calculations [28]. The calculation by Bertsch et al. [6] based on the tight-binding elec-

M. J. PUSKA AND R. M. NIEMINEN

tron structure of the C_{60} molecule gives $\alpha(\omega=0)=250a_0^3$, whereas the LDA calculation by Pederson and Quong [29] results in $542a_0^3$, which is quite close to our result. The static polarizabilities can be compared with the classical result $\alpha(\omega=0)=R^3$ for a conducting sphere. The use of the sphere radius (calculated from the positions of the C nuclei) $R=6.7a_0$ gives $\alpha(\omega=0)=300a_0^3$. Our larger polarizability can be qualitatively explained by the valence-electron density extending beyond the molecule radius.

Figure 3 shows the imaginary part of the dynamic polarizability of the jellium shell with 250 electrons. The polarizability is calculated using a small imaginary part of $\varepsilon=0.1$ eV in the energy in order to broaden the (single-particle) absorption peaks to become manageable in practical calculations. At low energies below 10 eV, there is one noticeable peak around 4 eV. The spectrum is dominated by a sharp peak around 13 eV. Between 15 and 22 eV, there are several smaller peaks. Moreover, at higher energies there is a broad hump around 35 eV.

The peak at 13 eV and the hump at 35 eV correspond to collective excitations of electrons. A similar structure has been noted for jellium spheres mimicking small metallic clusters [14,15]. The hump at the high energies corresponds to bulk-plasmon excitations. Indeed, the bulk-plasma frequency for electron gas with $r_s=1.2a_0$ is $\omega_p=35.9$ eV. The strong peak at 13 eV is a surface plasmon mode, which is, similarly to the case of jellium spheres, shifted to lower energies from its classical Mie-theory value of

$$\omega_{SP}=\omega_p/\sqrt{3}=20.7 \text{ eV} .$$

The peak at 4 eV corresponds to single-particle excitations from the highest occupied states and the narrow peaks between 15- and 22-eV excitations from the $n=2$ to $n=3$ states and from $n=1$ (σ) to $n=2$ (π) states.

The theoretical result given in Fig. 3 can be compared with those obtained by photoionization measurements [7] or by electron energy-loss spectroscopy [30] (EELS). Hertel et al. [7] found, using synchrotron radiation, a strong resonance in the photoion yield at about 20 eV with a full width at half maximum (FWHM) of about 10

eV. Hertel et al. analyzed their data for the photoion yield by factorizing it to the product of resonance excitation and autoionization probabilities. The former is directly proportional to the imaginary part of the polarizability of the C_{60} molecule. In addition, Hertel et al. found the imaginary part of the polarizability by applying the Clausius-Mossotti relation with complex dielectric constant measured [30] by electron energy-loss spectroscopy. These two different methods give results in good agreement with each other. Especially, there exist low peaklike structures at 10, 13, 17, and 21 eV. The positions of the 13- and 17-eV structures compare well with the peak structure in our results shown in Fig. 3. On the other hand, while we find peaks around 10 and 21 eV, their relative amplitudes are much smaller than in the experiments. Moreover, the measured resonance extends to higher photon energies than in our calculations. According to the photoion yield measurements, the absorption rises after the giant resonance again above 32 eV. Unfortunately, Hertel et al. [7] did not measure above 35 eV, and it is not clear if this rise corresponds to the bulk-plasmon-type resonance predicted by our model.

The EELS spectra [30] show prominent peaks at 6 and 26 eV. Following the work on graphite [31], the peak at 6 eV has been interpreted as collective excitations related to the transitions between π states, and the peak at 26 eV as a bulk-plasmon-type excitation of all σ and π electrons. The EELS spectra are, however, proportional to the loss function $\text{Im}(-1/\epsilon)$, where ϵ is the complex frequency-dependent dielectric function. As also shown by Hertel et al. [7], the giant resonance peak in the imaginary part of the polarizability is shifted in the loss function to higher energies. According to our calculations, the Mie-type resonance at 13 eV shown in Fig. 3 corresponds to a peak in the loss function at 26 eV.

Bertsch et al. [6] have calculated the oscillator strength for the C_{60} molecule using a valence-electron structure from the tight-binding model. They used the linear-response theory and accounted for the electron-electron interactions by the random-phase theory, which is close to the TD-DFT used in our work. The main differences of the approach of Bertsch et al. compared to ours are their omission of the continuum states and the electron exchange and correlation. Bertsch et al. found a collective giant resonance in the absorption around 22 eV, i.e., at higher energies than our double peak. They also used in the explanation of their results a jelliumlike model. Contrary to our results, they obtain for their model a single strong and narrow peak around 16 eV. The difference from our self-consistent result may also be due to different parameters of the shell.

B. Xe and Ba inside C_{60}

We have calculated the electronic structures and response functions for XeC_{60} and BaC_{60} molecules. In order to have closed electronic shell structures for the TD-DFT, it is necessary to use a jellium shell with 248 electrons for BaC_{60}. The resulting electron level scheme corresponding to the jellium-shell induced states remains similar to that shown in Fig. 1 for the pure jellium shell.
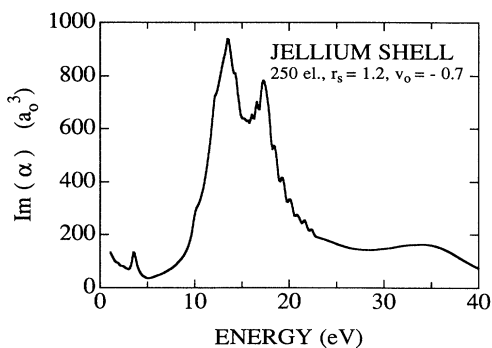

FIG. 3. Imaginary part of dynamic polarizability of the jellium shell with 250 electrons. The imaginary part is proportional to the photoabsorption cross section [Eq. (3)]. The driving frequency has a constant imaginary part of 0.2 eV.

The atom in the center of the jellium shell induces states which can be distinguished from the jellium-shell states by investigating the energy-level scheme or by noting that the wave functions of these states are clearly localized inside the jellium shell. This is true also for atom-induced states with eigenenergies within the jellium-shell energy band. In this way we find that the Xe atom preserves its closed electron shell structure and neutrality within the jellium, whereas Ba donates its uppermost s electrons to the jellium shell, appearing in the charge state Ba^{2+}. This kind of electron structure is in agreement with *ab initio* calculations [32].

With our spherical model, it is easy to study how the photoabsorption properties are changed when a free atom is surrounded by the C$_{60}$ carbon cage. This is especially interesting in the case of the so-called resonance absorption [33], in which typically a $4d$ or $5d$ core electron of a lanthanide or an actinide atom is excited to continuum, in which the final-state density is enhanced due to a $4f$ or $5f$ resonance. Above the threshold energy the photoabsorption cross section typically has a broad peak. If the atom is surrounded by other atoms, i.e., it is in a solid environment or a part of a molecule, the hybridization of the final atomic state with the states of the environment as well as the ligand field effects are expected to change the resonance absorption characteristics [16]. In this work we predict the effects of the C$_{60}$ carbon cage on the resonance absorption of $4d$ electrons of Xe and Ba atoms.

Figures 4 and 5 show the photoabsorption cross sections for free Xe and Ba atoms as well as for these atoms placed inside the C$_{60}$ molecule. The results for the free Ba and Xe atoms are in good agreement with previous TD-DFT [11,12] and other type of calculations [13]. It can be seen that the introduction of the jellium shell mimicking the carbon cage strongly suppresses the resonances and introduces weak oscillations. The suppression and the oscillations can be understood in terms of the overlap between the initial $4d$ and final scattering states. The initial $4d$ state is well localized and it is nearly unaffected by the introduction of the jellium shell. In the case of the scattering states the jellium shell causes more nodes to the wave functions because they have to be
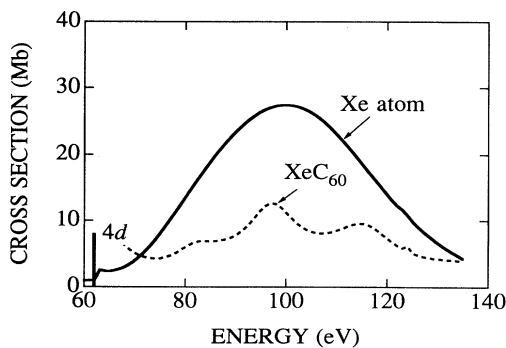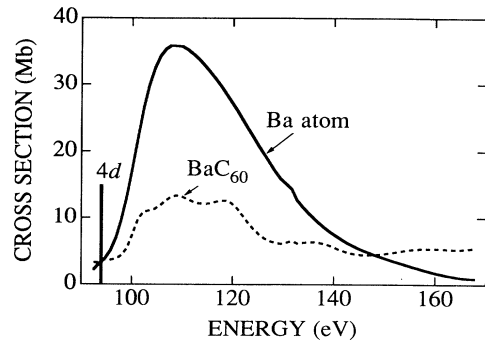

FIG. 5. Same as Fig. 4, but for Ba.

orthogonal to the two bound f states. This decreases the overlap integral. Even more important is that the scattering states have to be transmitted over the potential well due to the cage. The transmission probability decreases with decreasing energy, and the overlap and the absorption cross section are suppressed. Moreover, the transmission probability oscillates as a function of the electron energy. These oscillations are seen in the absorption cross section. As a matter of fact, the density of the scattering states also clearly shows these effects. When the jellium shell is introduced, the f resonance peak at low energies is remarkably narrowed (for Ba the FWHM decreases from about 1 to 0.5 eV). The density of states is strongly suppressed at energies around 10 eV from the bottom of the conduction band upwards, beyond which it oscillates as a function of energy. A suppression of the resonance photoabsorption cross section similar to the present ones has been previously seen by Zangwill and Liberman [16]. They studied the effects of the solid environment on the absorption above the $5d$ threshold of uranium by a model in which one uranium atom is embedded in the center of a jellium sphere. Wendin [34] has also seen the oscillations in the photoabsorption cross section using a non-self-consistent model with a spherical shell.

The carbon-cage-induced oscillations in the photoabsorption cross section have a counterpart in the extended x-ray absorption fine-structure (EXAFS) measurements for solid-state systems [35]. In the simplest picture of EXAFS, the emitted photoelectron is scatterred by the nearest-neighbor atoms back to the emitter, which contributes to the final state. As a result, oscillations in the photoionization cross section occur as a function of the photoelectron kinetic energy. Omitting multiple scattering, one can show that the oscillating modulation has the form [35]

$$-k^{-1}\sum_i A_i(k)\sin[2kR_i + \phi_i(k)] \ , \tag{7}$$

where k is the wave vector of the photoelectron, the summation is over the neighboring atomic shells, A_i is the backscattering amplitude associated with the ith shell, R_i the distance from the emitter to the ith shell, and ϕ_i the phase factor depending on the phase shifts for the emitter and scatterer potentials. Equation (7) can explain even quantitatively the oscillations seen in the calculated photoabsorption cross sections for Xe and Ba. Namely, om-

FIG. 4. Photoabsorption cross section for the free Xe atom (solid line) and for Xe inside the C$_{60}$ molecule (dashed line). The threshold energy for excitation from the $4d$ level is given by a vertical line.

itting the phase factor ϕ_i and using the carbon-cage radius for R_i, Eq. (7) predicts correctly the positions of the oscillations seen, for example, in Fig. 5 for Ba above photon energies of 110 eV.

V. SUMMARY

We have constructed a simple model, which is able to describe semiquantitatively many features of the electron structure of the C_{60} molecule. Within this model we have been able to calculate the photoabsorption cross section of the C_{60} molecule using the time-dependent density-functional theory. The theory reproduces the giant absorption resonance including some of its finer details. However, the width of the calculated resonance is smaller than that deduced from synchrotron or EELS measurements. We predict the effects due to the carbon cage on the $4d$ resonance absorption of the Xe and Ba atoms inside the C_{60} molecule. The cage suppresses the absorption cross section and causes a weakly oscillating structure as a function of energy.

[1] S. Satpathy, Chem. Phys. Lett. **130**, 545 (1986).
[2] S. Saito and A. Oshiyama, Phys. Rev. Lett. **66**, 2637 (1991).
[3] J. H. Weaver *et al.*, Phys. Rev. Lett. **66**, 1741 (1991).
[4] P. A. Heiney *et al.*, Phys. Rev. Lett. **66**, 2911 (1991).
[5] O. Gunnarsson, S. Satpathy, O. Jepsen, and O. K. Andersen, Phys. Rev. Lett. **67**, 3002 (1991).
[6] G. F. Bertsch *et al.*, Phys. Rev. Lett. **67**, 2690 (1991).
[7] I. V. Hertel *et al.*, Phys. Rev. Lett. **68**, 784 (1992).
[8] J. R. Heath *et al.*, J. Am. Chem. Soc. **107**, 7779 (1985).
[9] Y. Chai *et al.*, J. Chem. Phys. **95**, 7564 (1991).
[10] M. J. Stott and E. Zaremba, Phys. Rev. A **21**, 12 (1980).
[11] A. Zangwill and P. Soven, Phys. Rev. A **21**, 1561 (1980).
[12] A. Zangwill and P. Soven, Phys. Rev. Lett. **45**, 204 (1980).
[13] M. Kutzner, Z. Altun, and H. P. Kelly, Phys. Rev. A **41**, 3612 (1990).
[14] W. Ekardt, Phys. Rev. Lett. **52**, 1925 (1984); Phys. Rev. B **32**, 1961 (1985).
[15] M. J. Puska, R. M. Nieminen, and M. Manninen, Phys. Rev. B **31**, 3486 (1985).
[16] A. Zangwill and D. A. Liberman, Phys. Rev. B **36**, 6705 (1987).
[17] P. J. Benning *et al.*, Phys. Rev. B **44**, 1962 (1991).
[18] M. B. Jost *et al.*, Phys. Rev. B **44**, 1966 (1991).
[19] J. L. Martins, N. Troullier, and J. H. Weaver, Chem. Phys. Lett. **180**, 457 (1991).
[20] N. D. Lang and W. Kohn, Phys. Rev. B **1**, 4555 (1970).
[21] J. P. Perdew and R. Monnier, Phys. Rev. Lett. **37**, 1286 (1976).

[22] C. O. Almbladh and U. von Barth, Phys. Rev. B **13**, 3309 (1976).
[23] We use the local exchange-correlation functional based on the results by D. M. Ceperley and B. J. Alder, Phys. Rev. Lett. **45**, 566 (1980), and the parametrized form given by J. P. Perdew and A. Zunger, Phys. Rev. B **23**, 5048 (1981).
[24] For a review, see R. O. Jones and O. Gunnarsson, Rev. Mod. Phys. **61**, 689 (1989).
[25] J. A. Zimmermann *et al.*, J. Chem. Phys. **94**, 3556 (1991).
[26] D. L. Lichtenberger *et al.*, Chem. Phys. Lett. **176**, 203 (1991).
[27] H. Ajie *et al.*, J. Phys. Chem. **94**, 8630 (1990).
[28] P. W. Fowler, P. Lazzeretti, and R. Zanasi, Chem. Phys. Lett. **165**, 79 (1990).
[29] M. R. Pederson and A. A. Quong, Bull Am. Phys. Soc. **37**, 766 (1992).
[30] J. H. Sohmen, J. Fink, and W. Krätschmer, Z. Phys. B **86**, 87 (1992).
[31] U. Diebold *et al.*, Surf. Sci. **197**, 430 (1988).
[32] A. H. H. Chang, W. C. Ermler, and R. M. Pitzer, J. Chem. Phys. **94**, 5004 (1991).
[33] See, for example, Giant Resonances in Atoms, Molecules, and Solids, Vol. 151 of *NATO Advanced Study Institute, Series B: Physics*, edited by J. P. Connerade, J. M. Esteva, and R. C. Karnatak (Plenum, New York, 1987).
[34] G. Wendin (private communication).
[35] See, for example, D. P. Woodruff and T. A. Delchar, *Modern Techniques of Surface Science* (Cambridge University Press, Cambridge, 1986), p. 122.